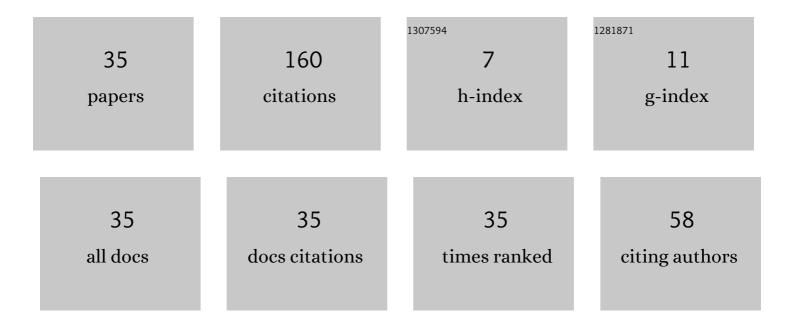
Ali Kiraci

List of Publications by Year in descending order

Source: https://exaly.com/author-pdf/9128432/publications.pdf Version: 2024-02-01



ΔιιΚιρλοι

#	Article	IF	CITATIONS
1	Temperature Dependence of the Raman Frequency, Damping Constant and the Activation Energy of a Soft-Optic Mode in Ferroelectric Barium Titanate. Ferroelectrics, 2012, 432, 14-21.	0.6	21
2	Calculation of the Damping Constant and the Relaxation Time for the Soft-Optic and Acoustic Mode in Hexagonal Barium Titanate. Ferroelectrics, 2012, 437, 137-148.	0.6	16
3	Temperature dependence of the damping constant and the relaxation time close to the tetragonal-cubic phase transition in SrZrO3. Journal of Molecular Structure, 2017, 1128, 51-56.	3.6	12
4	Calculation of the Raman frequency and the damping constant of a coupled mode in the ferroelectric and paraelectric phases in KH ₂ PO ₄ . Physica Status Solidi (B): Basic Research, 2010, 247, 927-936.	1.5	10
5	Temperature dependence of the polarization and the dielectric constant near the paraelectric-ferroelectric transitions in BaTiO3. Journal of Molecular Modeling, 2013, 19, 3925-3930.	1.8	8
6	Damping constant and the relaxation time calculated for the lowest-frequency soft mode in the ferroelectric phase of Cd2Nb2O7. Optik, 2016, 127, 11497-11504.	2.9	8
7	Analysis of the specific heat and the free energy of [N(CH3)4]2ZnBr4 close to the ferro-paraelastic phase transition. Phase Transitions, 2019, 92, 249-258.	1.3	8
8	Raman linewidths calculated as a function of temperature in NaNO ₂ . Physica Status Solidi (B): Basic Research, 2009, 246, 1124-1131.	1.5	7
9	CALCULATION OF THE DAMPING CONSTANT AND ACTIVATION ENERGY FOR RAMAN MODES IN (NH ₄) ₂ SO ₄ . International Journal of Modern Physics B, 2011, 25, 2063-2080.	2.0	7
10	Damping Constant (Linewidth) and the Relaxation Time of the Brillouin LA Mode for the Ferroelectric-Paraelectric Transition in PbZr1– <italic>x</italic> Ti <italic>x</italic> O3. IEEE Transactions on Ultrasonics, Ferroelectrics, and Frequency Control, 2016, 63, 1647-1655.	3.0	7
11	Damping Constant Calculated as a Function of Temperature for the Tetragonal Raman Mode Close to the Paraelectric-Ferroelectric Transition in BaTiO ₃ . Ferroelectrics, 2013, 450, 93-98.	0.6	6
12	Temperature dependence of the polarization, dielectric constant, damping constant and the relaxation time close to the ferroelectric-paraelectric phase transition in LiNbO3. Optik, 2017, 132, 183-191.	2.9	6
13	Calculation of the raman frequency, damping constant (Linewidth) and the relaxation time near the tetragonal-cubic transition in PbTiO3. Optik, 2017, 142, 311-319.	2.9	6
14	A phenomenological study on ferroelectric pyridinium tetrafluoroborate (C5NH6) BF4. Thermochimica Acta, 2019, 680, 178371.	2.7	6
15	Pressureâ€dependent Raman modes near the cubicâ€ŧetragonal transition in strontium titanate. Journal of the American Ceramic Society, 2018, 101, 1344-1355.	3.8	5
16	Damping constant and the inverse relaxation time calculated as a function of pressure using the X-ray diffraction data close to the cubic-tetragonal phase transition in SrTiO3. Ferroelectrics, 2019, 551, 143-151.	0.6	5
17	Calculation of the damping constant and the order parameter for the lattice mode in ferroelectric PbTiO <inf>3</inf> ., 2013, .		4
18	Analysis of the integrated intensity of the central peaks calculated as a function of temperature in the ferroelectric phase of lithium tantalate. Thermal Science, 2018, 22, 221-227.	1.1	4

Ali Kiraci

#	Article	IF	CITATIONS
19	Order–disorder transition in the ferroelectric LiTaO3. Ferroelectrics, 2019, 551, 235-244.	0.6	3
20	The Important Role of N(2)(CH3)4 Ion in the Phase-Transition Mechanism of [N(CH3)4]2ZnBr4. IEEE Transactions on Ultrasonics, Ferroelectrics, and Frequency Control, 2020, 67, 1053-1058.	3.0	3
21	A phenomenological study on ferroelectric β-glycine. Ferroelectrics, 2021, 572, 277-286.	0.6	3
22	A phenomenological study on ferroelastic KH3(SeO3)2 and KD3(SeO3)2. Materials Research Bulletin, 2021, 143, 111472.	5.2	2
23	Calculation of the Infrared Frequencies as a Function of Temperature Using the Volume Data in the Ferroelectric Phase of NaNO ₂ . Ferroelectrics, 2014, 460, 149-156.	0.6	1
24	Phenomenological approaches on the Nd3+ doped ferroelectric LaBGeO5. Ferroelectrics, 2021, 572, 13-26.	0.6	1
25	Calculation of the spin-lattice relaxation time and the activation energy near the IV–III phase transition in pyridinium fluorosulfonate (C ₅ NH ₆)FSO ₃ . Ferroelectrics, 2022, 589, 45-54.	0.6	1
26	Temperature dependence of the Brillouin frequency shift and the linewidth of the LA mode in the ferroelectric phase of PZT-x (PbZr <inf>1−x</inf> Ti <inf>x</inf> O <inf>3</inf>). , 2015, , .		0
27	Pressure dependence of the Raman frequency calculated from the volume data close to the ferroelectric-paraelectric transition in PbTiO ₃ . Ferroelectrics, 2017, 520, 245-255.	0.6	0
28	Calculation of the frequency shifts and damping constant for the Raman modes (A\$_{1g}\$, B\$_{1})\$ near the tetragonal-cubic transition in SrTiO\$_{3}\$. Turkish Journal of Physics, 2017, 41, 526-535.	1.1	0
29	Raman wavenumbers calculated as a function of pressure from the mode Grüneisen parameter of PZT (x=0.48) ceramic close to the monoclinic-cubic transition. Journal of Advanced Dielectrics, 2019, 09, 1950039.	2.4	0
30	A thermodynamic study on PbZr0.52Ti0.48O3 ceramic close to the tetragonal-cubic transition. Journal of the Australian Ceramic Society, 2020, 56, 79-90.	1.9	0
31	Phenomenological Study of Manganese Antimonite Close to the Néel Temperature. IEEE Magnetics Letters, 2021, 12, 1-5.	1.1	0
32	Damping constant, dielectric susceptibility, inverse relaxation time and the activation energy calculated as a function of temperature from the Raman frequency for the rhombohedral-tetragonal phase transition in BaCeO3. Balıkesir Üniversitesi Fen Bilimleri Enstitüsü Dergisi, 0, , 77-83.	0.3	0
33	Calculation of the Relaxation Time and the Activation Energy Close to the Lower Phase Transition in Imidazolium Perchlorate. Journal of Basic & Applied Sciences, 0, 17, 79-86.	0.8	0
34	Analysis of the specific heat and the free energy and calculation of the entropy and the internal energy of [N(CH3)4]2MnBr4 close to the phase transition. Ferroelectrics, 2021, 583, 1-11.	0.6	0
35	Analysis and mathematical computation of some dynamic functions for the guanidine zinc sulfate. Ferroelectrics, 2021, 584, 39-50.	0.6	0